LETTER

NJC
www.rsc.org/njc

Engineering of an electronically decoupled difluoroindacene-pyrene dyad possessing high affinity for DNA

James P. Rostron,[a] Gilles Ulrich,[b] Pascal Retailleau,[c] Anthony Harriman*[a] and Raymond Ziessel*[b]

[a] *Molecular Photonics Laboratory, School of Natural Sciences (Chemistry), Bedson Building, University of Newcastle, Newcastle upon Tyne, UK NE1 7RUE-mail: anthony.harriman@ncl.ac.uk; Fax: +44 (0)191 222 8664; Tel: +44 (0)191 222 8660*

[b] *Laboratoire de Chimie Moléculaire, École de Chimie, Polymères, Matériaux (ECPM), Université Louis Pasteur (ULP), 25 rue Becquerel, 67087 Strasbourg Cedex 02, France. E-mail: ziessel@chimie.u-strasbg.fr; Fax: +33 390242689; Tel: +33 390242689*

[c] *Laboratoire de Cristallochimie, ICSN - CNRS, Bât 27-1 avenue de la Terrasse, 91198 Gif-sur-Yvette Cedex, France*

Received (in Montpellier, France) 31st May 2005, Accepted 4th August 2005
First published as an Advance Article on the web 1st September 2005

DOI: 10.1039/b507585h

A highly fluorescent dual-dye, comprising 4,4-difluoro-8-(aryl)-1,3,5,7-tetramethyl-2,6-diethyl-4-bora-3a,4a-diaza-*s*-indacene and 1-pyrenyl fragments linked orthogonally at the pseudo-*meso* position, displays a wide choice of excitation wavelengths due to intramolecular energy transfer and undergoes efficient fluorescence quenching when bound to double-stranded DNA.

Despite intensive investigation for several decades, there is still an urgent need to identify highly luminescent probes for specific applications in medical diagnostics, immuno-histochemistry and molecular biology.[1,2] Several sophisticated design elements have been reported. For example, oligonucleotide probes carrying a fluorophore and an intercalating unit have been prepared that signal the presence of their target sequence by modulation of the fluorescence yield because intercalation curtails intramolecular excitation energy transfer.[3] Likewise, homogeneous fluorescence assay methods have been successfully applied to the detection of a specific sequence of oligopeptides and single base alterations.[4] Many different fluorescence markers for specific DNA sequences are now known, including cationic dyes[5] and aromatic polycycles such as benzopyrene, anthracene and pyrene.[6] These intercalators are characterised by high fluorescence quantum yields, before or after binding to DNA, but rather small Stokes shifts. The latter finding is a particular problem for fluorescence microscopy and flow cytometry.

In searching for neutral chromophores that are chemically robust and display excellent photophysical properties, the 4,4-difluoro-4-bora-3a,4a-diaza-*s*-indacene (bodipy™) class of dyes looks to be particularly attractive.[7] In part, this is because substitution at the pseudo-*meso* position is facile.[8] In order to circumvent the problem of a small Stokes shift, it is noticeable that the dye exhibits a weak absorption transition around 380 nm. This band is situated where pyrene is known to emit, such that there exists the strong possibility to effect efficient intramolecular singlet energy transfer from pyrene to bodipy.[9] As such, the bodipyrene dye **1** and the reference compound **2** were synthesised. It was anticipated that the pyrene unit might intercalate into DNA and that the likely orthogonal geometry would prevent strong electronic communication between the two units.

Preparation of **1** was carried out by condensation of 1-pyrenecarboxaldehyde with kryptopyrrole under acidic conditions. Successive oxidation with DDQ and treatment with $BF_3 \cdot Et_2O$ in basic conditions afforded the target in an overall yield of 25%. Compound **2** was synthesised in 95% yield, as indicated in Scheme 1, by cross-coupling between the iodo-substituted bodipy dye and 4-ethynyltoluene, with Pd(0). Both dyes were spectroscopically characterised including ^{11}B NMR and positive mode FAB-MS: δ 4.08 (t, $J_{B,F} = 33.7$ Hz), 505.2 $[M + H]^+$ for **1** and 3.86 (t, $J_{B,F} = 32.7$ Hz), 495.1 $[M + H]^+$ for **2**.

The single-crystal molecular structure of **1**† confirms the quasi-orthogonal arrangement between the mean planes of the indacene and pyrene units (Fig. 1). The central six-membered ring lies coplanar to the two adjacent five-membered rings [the maximum deviation from planarity for the 12 atoms belonging to the indacene unit being 0.025(3) Å], ensuring good π-electron delocalisation. Pronounced double-bond character is apparent for C4A–N1A and C4B–N1B [1.346(6) Å], whereas classical single-bond features are found for C5A–N1A and C5B–N1B [1.398(3) Å].

Both compounds are electroactive and close examination of the redox behaviour allows assignment of the various oxidation and reduction processes. In both cases, reversible formation of the radical cation of the bodipy unit is found at +1.02 V *vs.* SSCE and of the radical anion at −1.20 V *vs.* SSCE.[8] The additional reversible redox processes found for **1** at +1.48 and −1.96 V *vs.* SSCE are assigned to formation of the radical cation and anion, respectively, localised on the pyrene fragment.

The absorption spectrum recorded for **1** in methanol solution is as might be expected for a 1 : 1 molar mixture of the corresponding model compounds, indicating that electronic interaction between the subunits is rather small. There is a strong absorption centred at 528 nm ($\varepsilon = 73\,000$ M^{-1} cm^{-1}) which can be assigned to the $S_0 \rightarrow S_1$ (π–π*) transition of the bodipy fragment.[10] Additional intense absorptions are found at 340 nm ($\varepsilon = 39\,000$ M^{-1} cm^{-1}) and 325 nm ($\varepsilon = 26\,100$ M^{-1}

† Crystal data for **1**: $C_{34}H_{34}BF_2N_3O_2$, $M = 565.45$, triclinic, $a = 7.266(4)$, $b = 12.168(3)$, $c = 17.628(4)$ Å, $\alpha = 100.33$, $\beta = 90.79(2)$, $\gamma = 104.64°$, $V = 1480.6(10)$ Å^3, $T = 293(2)$ K, space group $P\bar{1}$, $Z = 2$, $\mu = 0.087$ mm^{-1}, 6784 reflections measured, 4181 unique ($R_{int} = 0.0271$), R_1 $[I > 2\sigma(I)] = 0.0740$, w$R_2$ (all data) = 0.2367. CCDC reference number 263269. See http://dx.doi.org/10.1039/b507585h for crystallographic data in CIF or other electronic format.

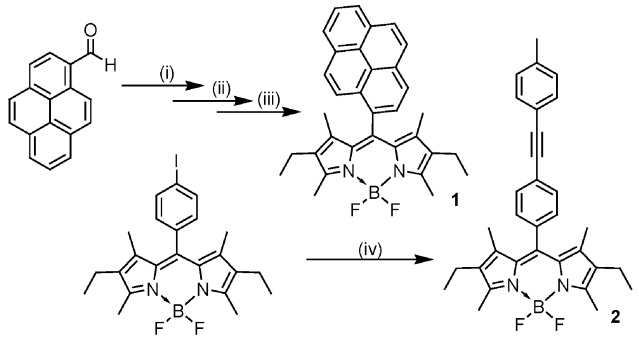

Scheme 1 (i) 1,3-Dimethyl-4-ethylpyrrole, *p*-TsOH, CH_2Cl_2, rt; (ii) DDQ; (iii) $BF_3 \cdot Et_2O$, TEA; (iv) 4-ethynyltoluene, THF–*i*Pr_2NH, $Pd(PPh_3)_2Cl_2$ (6 mol%), CuI (10 mol%), rt.

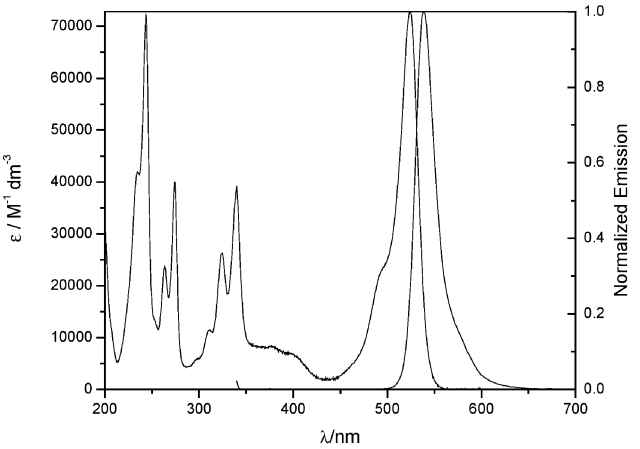

Fig. 2 Absorption and fluorescence spectra recorded for **1** in methanol solution.

cm^{-1}) that are associated with the pyrene unit (Fig. 2). The reference compound **2** shows appropriate transitions that help in the assignment. In addition, both dyes are strongly fluorescent in methanol solution (Fig. 2). Emission maxima (λ_{em}) are found at 540 and 542 nm, respectively, for **1** and **2**, whilst the fluorescence quantum yields (ϕ_{flu}) measured in deoxygenated methanol solution are 0.90 for **1** and 0.87 for **2**. Fluorescence decay profiles were found to be mono-exponential at all excitation and detection wavelengths and correspond to excited state lifetimes of 7.0 and 5.5 ns, respectively, for **1** and **2**. Emission is clearly from the first-excited singlet state associated with the bodipy unit, for which the Stokes shift is only *ca.* 600 cm^{-1}.

The fluorescence excitation spectrum was found to be in excellent agreement with the absorption spectrum recorded over the visible and near-UV regions. In particular, photons absorbed by the pyrene unit in **1** are transferred quantitatively to the bodipy fragment. No fluorescence could be detected from the pyrene-like unit within the range 380–500 nm. Since the fluorescence quantum yield and singlet lifetime measured for pyrene under these conditions are 0.76 and 140 ns, respectively, it can be argued that the rate constant for intramolecular excitation energy transfer in **1** is $>10^{10}$ s^{-1}. This value is entirely consistent with the calculated rate constant for Förster-type energy transfer from pyrene to the second-excited singlet state localised on the bodipy unit. Overall, this has the effect of increasing the energy gap between excitation and fluorescence maxima to 10 900 cm^{-1}.

In addition to providing for a substantial improvement in the optical properties, the pyrene unit offers the possibility of anchoring the dye close to double-stranded DNA.[11] Thus, addition of small aliquots of **2** in DMSO to an aqueous solution of DNA (pH 7, 0.005 M Na_2SO_4) resulted in the appearance of fluorescence characteristic of a bodipy dye. In marked contrast, fluorescence from **1** was extensively quenched by the presence of DNA. Very little fluorescence could be detected at high ratios of DNA, measured in terms of phosphate groups (P), to dye (D) (P/D = 20) but emission began to appear as the concentration of free dye increased (Fig. 3 and 4). This observation was found to hold true for excitation into both bodipy and pyrene units.

Time-resolved fluorescence studies following direct excitation into the bodipy unit (P/D = 10) showed that the decay profiles were dual-exponential. The averaged fluorescence lifetimes were 7.0 ns and 140 ps. Raising the P/D ratio caused an increase in the relative contribution of the shorter lived component but did not change either lifetime. As such, the shorter lifetime can be attributed to dye bound to DNA whereas the longer lifetime can be assigned to dye free in solution or loosely bound to the duplex. Similar behaviour was found for excitation into the pyrene subunit, although no fluorescence from pyrene could be detected. At very low loading (P/D > 60), the

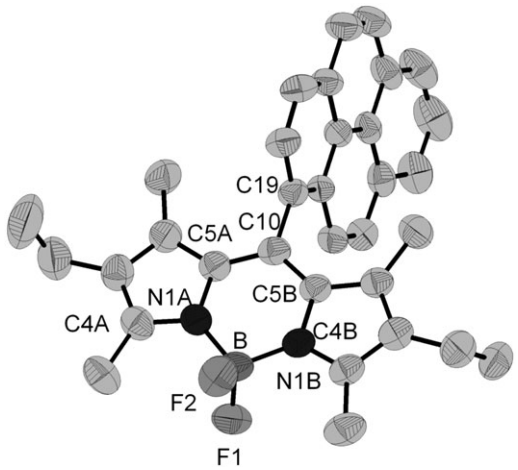

Fig. 1 ORTEP view for **1** showing the atom-labelling scheme. Thermal ellipsoids are plotted at the 30% level. B–N1A, B–N1B, B–F1, B–F2 and C10–C19 bond lengths are 1.538(6), 1.540(6), 1.393(5), 1.391(5) and 1.496(5) Å and the N–B–N, F–B–F, and N–B–F angles are 107.3(4), 108.6(3) and 110.0(3), 110.4(4), 109.7(4) and 110.6(3)°.

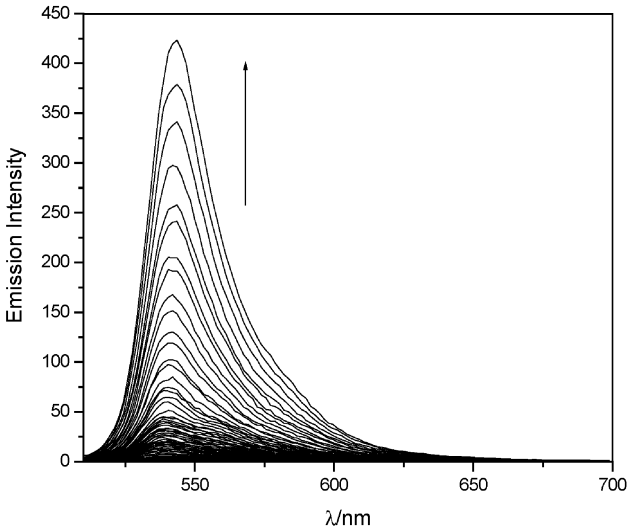

Fig. 3 Fluorescence spectral titration made for addition of **1** to DNA. The excitation wavelength was 495 nm and the concentration of DNA was 20 μM, measured in terms of base pairs. The background electrolyte was sodium sulfate (5 mM) in pH 7 buffer at a total ionic strength of 0.1 M.

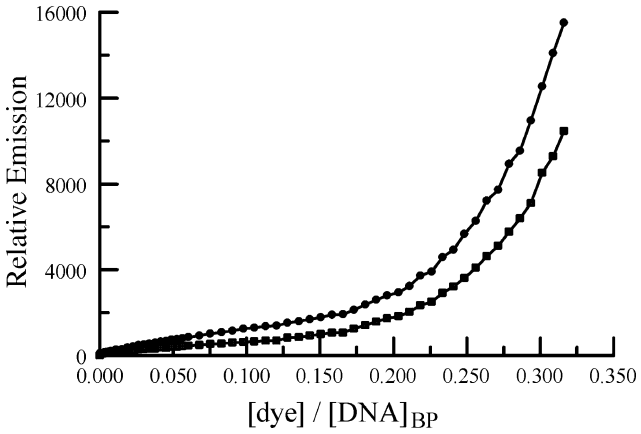

Fig. 4 A typical fluorescence spectral titration made for addition of **1** to DNA. Excitation was made into the pyrene (■) or bodipy (●) units. The concentration of DNA was measured in terms of base pairs. The background electrolyte was sodium sulfate (5 mM) in pH 7 buffer at a total ionic strength of 0.1 M.

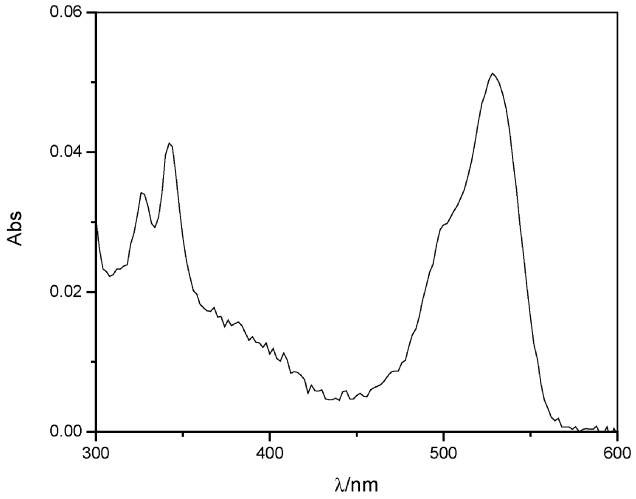

Fig. 5 Absorption spectrum recorded for **1** after binding to DNA at P/D = 50.

fluorescence lifetime was increased from 140 to 320 ps. There was a corresponding increase in the relative fluorescence yield.

Analysis over the full concentration range indicates that a minimum of three disparate types of dye is required to fit the data. In addition to free dye, there are two bound species. At high P/D, fluorescence is heavily quenched but still observable. As the P/D ratio decreases, the relative fluorescence yield decreases but is supplemented by dye free in solution. Under these latter conditions, bound dye is only weakly fluorescent.

The fluorescence titrations were considered in terms of a linear combination of fluorescence from free and both types of bound dye. For direct excitation into the bodipy unit, saturation binding occurs at a loading (n) of 5 base pairs. The same analysis made for excitation into the pyrene unit gives $n = 6$. This derived value is considered to be rather high for intercalation but could be consistent with binding in the major groove. Under these conditions, with $5 < P/D < 20$, the averaged association constant (K) for binding of **1** to double-stranded DNA is 4.3×10^6 M^{-1}. The same value was derived regardless of which unit was excited.

Association of **1** with DNA has little obvious effect on the fluorescence spectral profile, although the lifetime and quantum yield are greatly reduced. The absorption spectrum (Fig. 5), however, shows marked changes compared to that recorded in methanol. In particular, the $S_0 \rightarrow S_1$ transition associated with the bodipy unit is broadened, reduced in intensity and red-shifted by 5 nm after binding to DNA. The $S_0 \rightarrow S_2$ transition centred on the bodipy unit is enhanced, blue-shifted by 5 nm and broadened upon binding to the duplex. In contrast, absorption bands localised on the pyrene unit are little affected by the presence of DNA, apart from broadening. These spectral changes are inconsistent with intercalation of pyrene into the strand.[12] As such, it is suggested that **1** binds to the major groove on the DNA duplex. The driving force for association with DNA presumably arises from the hydrophobic effect since neither bodipy[13] nor pyrene[11] are water soluble. Packing in the major groove provides a facile way to minimise surface contact with water. Self-aggregation of bodipy-labelled gangliosides in micellar structures have previously been observed.[13]

The binding studies indicate that at low loading ($P/D > 20$) there is extensive quenching of the fluorescence from the bodipy unit. Relative to dye free in solution, this quenching effect corresponds to a 20-fold reduction in the excited state lifetime. At higher loadings ($P/D \approx 10$), there is a further reduction in the fluorescence yield and lifetime. This latter effect is most likely due to aggregation of the dye along the duplex, due to clustering. The bodipy units lack the functionality to intercalate between base pairs, although pyrene is known to do so.[11] For **1**, there is no evidence to suggest that intercalation occurs. Electrochemical studies show that the bodipy unit can be both oxidised and reduced at modest potentials. Allowing for the excitation energy of 2.28 eV, the excited state oxidation and reduction potentials, respectively, become −1.26 and +1.08 V *vs.* SSCE. There is considerable uncertainty about the reduction potentials of the nucleic acid bases in the duplex but it is well established that guanine ($E_{ox} \approx 1.1$ V *vs.* SSCE) is the more easily oxidised species[14] and cytosine ($E_{red} \approx -1.3$ V *vs.* SSCE) in the most easily reduced species.[15] Light-induced intrastrand electron transfer, therefore, might be responsible for the observed fluorescence quenching. If so, the close proximity between the reactants might offset the limited thermodynamic driving force. Intrastrand electron transfer between intercalated and surface-bound reagents has been observed previously[16] but in the absence of detailed information it is not possible to pursue this argument further.

The main interest in this class of dye stems from its facile synthesis and ready substitution. A vast range of derivatives could be anticipated with properties tuned to particular applications. These compounds are soluble in most organic solvents and are highly fluorescent. The large excitation/detection energy gap and high photostability favours their use in fluorescence microscopy.

In summary, **1** is representative of a new class of fluorescent dyes carrying a pyrene fragment. The room temperature fluorescence quantum yield approaches unity and no triplet state formation could be observed. Because the emitting state is π,π* in character, the fluorescence properties are relatively insensitive to changes in temperature or solvent polarity. Fluorescence is extinguished upon binding to double-stranded DNA. The binding constant is high but intercalation does not seem to play an important role in the association process. Instead, the dye appears to cluster in the major groove, without obvious sign of site selectivity. The molecular dimensions of **1** are such that a saturation number of five corresponds to complete occupancy of the major groove. At this point, the duplex is coated with a sheath of dye, leaving almost no space between adjacent dye molecules. It should be noted that the corresponding dye lacking the pyrene unit does not bind to DNA with reasonable affinity. Prolonged illumination into the DNA:dye conjugate does not lead to strand scission, as evidenced by gel electrophoresis.

A comment can now be made regarding the analytical use of **1** as a fluorescent sensor for DNA in solution. The sensor would be used in ratiometric mode with a known concentration

of **1** being slowly injected into parallel solutions, one of which contains DNA. The difference in fluorescence between the two samples is used for detection purposes. Under optimised conditions, it is easily possible to detect free **1** at a concentration of *ca.* 1 μM. On the basis of the above experiments, this translates to a total DNA concentration of *ca.* 20 μM, measured in terms of base pairs. The minimum volume that could be used is 1 μL and the average molar mass of DNA can be taken as being *ca.* 7×10^8 Da. This means that around 15 000 molecules of DNA could be measured with acceptable precision by this methodology.

We thank the CNRS, the Université Louis Pasteur, EPSRC and the University of Newcastle for financial support.

Experimental

Compound **1** was prepared by condensation of 1-pyrenecarboxaldehyde with two equivalents of kryptopyrrole in dichloromethane with catalytic amounts of *p*-TsOH. The resulting dipyrromethane was smoothly oxidised with DDQ, followed by complexation by $BF_3 \cdot Et_2O$ in basic conditions. Spectroscopic data: for **1**, ^{1}H NMR ($CDCl_3$): δ = 8.02–8.29 (m, 8H), 7.89 (d, 1H, ^3J = 7.7 Hz), 2.60 (s, 6H), 2.23 (q, 4H, ^3J = 7.5 Hz), 0.92 (t, 6H, ^3J = 7.5 Hz), 0.78 (s, 6H); ^{13}C NMR: δ = 153.9, 138.9, 138.5, 132.8, 131.6, 131.3, 131.1, 130.3, 129.5, 128.7, 128.2, 127.3, 126.4, 126.2, 125.6, 125.5, 125.3, 124.6, 124.5, 124.4, 17.4, 14.6, 12.6 , 11.1; UV-Vis (CH_2Cl_2): λ nm (ε, M^{-1} cm^{-1}) = 529 (83 000), 342 (45 600), 327 (30 100), 276 (48 300), 265 (29 500), 245 (82 000); for **2**, ^{1}H NMR ($CDCl_3$): δ = 7.47 (ABsys, 4H, J_{AB} = 8.1 Hz, $\nu_0\delta$ = 74.3 Hz), 7.33 (ABsys, 4H, J_{AB} = 8.1 Hz, $\nu_0\delta$ = 54.5 Hz), 2.54 (s, 6H), 2.31 (q, 4H, ^3J = 7.6 Hz), 1.37 (s, 6H), 0.99 (t, 6H, ^3J = 7.5 Hz); ^{13}C NMR ($CDCl_3$): δ = 154.4, 139.8, 139.2, 138.6, 136.0, 133.3, 132.6 (CH), 131.9 (CH), 130.9, 129.6 (CH), 128.9 (CH), 124.5, 120.2, 91.2 (C≡C), 88.5 (C≡C), 21.9 (CH_3), 17.5 (CH_2), 14.9 (CH_3), 12.9 (CH_3), 12.3 (CH_3); UV-Vis (CH_2Cl_2): λ nm (ε, M^{-1} cm^{-1}) = 527 (56 100), 357 (9 100), 283 (41 800), 296 (36 400), 253 (65 600), 243 (57 500).

Absorption spectra were recorded with a Hitachi U-3310 spectrophotometer while fluorescence spectra were recorded with a Jobin-Yvon Fluorolog tau-3 spectrometer. Samples were thermostatted at 20 °C. Titrations were made by adding at least 30 aliquots of titrant to a fixed volume of reagent. Fluorescence lifetimes were measured with the Fluorolog, after deconvolution of the instrumental response function. Cyclic voltammetry was made with a HCH Electrochemical Analyser using a conventional 3-electrode set-up.

References

1 B. Valeur, *Molecular Fluorescence: Principles and Applications*, Wiley-VCH, Weinheim, Germany, 2002.
2 V. V. Didenko, *BioTechniques*, 2001, **31**, 1106.
3 K. Shinozuka, Y. Seto and H. Sawai, *J. Chem. Soc., Chem. Commun.*, 1994, 1377, and references cited therein.
4 A. Yamane, *Nucleic Acids Res.*, 2002, **30**, 97.
5 (*a*) B. P. Bowen and N. W. Woodbury, *Photochem. Photobiol.*, 2003, **78**, 582; (*b*) M. Kubista, B. Åkerman and B. Nordén, *Biochemistry*, 1987, **26**, 4545; (*c*) F. A. Tanious, J. M. Veal, H. Buczak, L. S. Ratmeyer and W. D. Wilson, *Biochemistry*, 1992, **31**, 3103.
6 (*a*) T. Meehan, H. Gamper and J. F. Becker, *J. Biol. Chem.*, 1982, **257**, 10479; (*b*) H.-C. Becker and B. Nordén, *J. Am. Chem. Soc.*, 1999, **121**, 11947; (*c*) U. B. Christensen and E. B. Pedersen, *Helv. Chim. Acta*, 2003, **86**, 2090; (*d*) A. Okamoto, T. Ichiba and I. Saito, *J. Am. Chem. Soc.*, 2004, **126**, 8364.
7 R. P. Haugland, *Handbook of Molecular Probes and Research Products*, Molecular Probes, Inc., Eugene, OR, 9th edn, 2002.
8 G. Ulrich and R. Ziessel, *J. Org. Chem.*, 2004, **69**, 2070.
9 M. Hissler, A. Harriman, A. Khatyr and R. Ziessel, *Chem. Eur. J.*, 1999, **5**, 3366.
10 J. Karolin, L. B.-A. Johansson, L. Strandberg and T. Ny, *J. Am. Chem. Soc.*, 1994, **116**, 7801.
11 R. Huber, T. Fiebig and H.-A. Wagenknecht, *Chem. Commun.*, 2003, 1878.
12 (*a*) N. E. Geacintov, T. Prusik and J. M. Khosrofian, *J. Am. Chem. Soc.*, 1976, **98**, 6444; (*b*) N. Cho and S. A. Asher, *J. Am. Chem. Soc.*, 1993, **115**, 6349.
13 F. Berström, I. Mikhalyov, P. Hägglöf, R. Wortmann, T. Ny and L. B.-Å. Johansson, *J. Am. Chem. Soc.*, 2002, **124**, 196.
14 (*a*) S. Steenken and S. V. Jovanovic, *J. Am. Chem. Soc.*, 1997, **119**, 617; (*b*) D. H. Johnston, C.-C. Cheng, K. J. Campbell and H. H. Thorp, *Inorg. Chem.*, 1994, **33**, 161; (*c*) V. Brabec, *Biophys. Chem.*, 1979, **9**, 289.
15 S. Steenken, J. P. Telo, H. M. Novais and L. P. Candeias, *J. Am. Chem. Soc.*, 1992, **114**, 4701.
16 A. Harriman, *Angew. Chem. Int. Ed.*, 1999, **38**, 945.